

1 Long timescale anti-directional rotation in *Drosophila* optomotor behavior

2

3 Omer Mano<sup>1</sup>, Minseung Choi<sup>2</sup>, Ryosuke Tanaka<sup>3</sup>, Matthew S. Creamer<sup>3</sup>, Natalia C.B. Matos<sup>3</sup>,  
4 Joseph Shomar<sup>4</sup>, Bara A. Badwan<sup>5</sup>, Thomas R. Clandinin<sup>2</sup>, Damon A. Clark<sup>1,3,4,6,#</sup>

5

6 1 – Department of Molecular, Cellular, and Developmental Biology, Yale University, New  
7 Haven, CT 06511, USA

8 2 – Department of Neurobiology, Stanford University, Stanford, CA 94305, USA

9 3 – Interdepartmental Neuroscience Program, Yale University, New Haven, CT 06511, USA

10 4 – Department of Physics, Yale University, New Haven, CT 06511, USA

11 5 – Department of Chemical Engineering, Yale University, New Haven, CT 06511, USA

12 6 – Department of Neuroscience, Yale University, New Haven, CT 06511, USA

13 # – Lead author: [damon.clark@yale.edu](mailto:damon.clark@yale.edu)

14

15 **Abstract**

16 Locomotor movements cause visual images to be displaced across the eye, a retinal slip that is  
17 counteracted by stabilizing reflexes in many animals. In insects, optomotor turning causes the  
18 animal to turn in the direction of rotating visual stimuli, thereby reducing retinal slip and  
19 stabilizing trajectories through the world. This behavior has formed the basis for extensive  
20 dissections of motion vision. Here, we report that under certain stimulus conditions, two  
21 *Drosophila* species, including the widely studied *D. melanogaster*, can suppress and even  
22 reverse the optomotor turning response over several seconds. Such ‘anti-directional turning’ is  
23 most strongly evoked by long-lasting, high-contrast, slow-moving visual stimuli that are distinct  
24 from those that promote syn-directional optomotor turning. Anti-directional turning, like the syn-  
25 directional optomotor response, requires the local motion detecting neurons T4 and T5; a subset  
26 of lobula plate tangential cells, CH cells, show involvement in these responses. Imaging from a  
27 variety of direction-selective cells in the lobula plate shows no evidence of dynamics that match  
28 the behavior, suggesting that the observed inversion in turning direction emerges downstream of  
29 the lobula plate. Further, anti-directional turning declines with age and exposure to light. These  
30 results show that *Drosophila* optomotor turning behaviors contain rich, stimulus-dependent  
31 dynamics that are inconsistent with simple reflexive stabilization responses.

32 **Intro**

33 Visual navigation requires active mechanisms to stabilize trajectories through the world. Insects  
34 exhibit an optomotor turning response, a behavior in which they rotate their bodies in the  
35 direction of visual patterns that rotate about them (Buchner, 1976; Götz and Wenking, 1973;

36 Hassenstein and Reichardt, 1956). This behavior is analogous to optomotor turning responses in  
37 fish (Clark, 1981) and the optokinetic response in mammals (Koerner and Schiller, 1972). In  
38 insects, this response is thought to be a course-stabilization mechanism that minimizes retinal  
39 slip, allowing animals to maintain their trajectory in the face of external or unexpected rotational  
40 forces (Götz and Wenking, 1973; Götz, 1975). For instance, if an insect attempts to walk in a  
41 straight line, it may slip and turn to the right. From the point of view of the insect, this turn is  
42 observed as optic flow rotating to the left. By responding to this leftward optic flow with a  
43 leftward turn, the insect can recover its original trajectory. The optokinetic response, similarly,  
44 acts to stabilize eye position relative to the visual scene, even as the head rotates (Schweigart et  
45 al., 1997).

46 In fruit flies, the optomotor response relies on well-characterized circuitry (Yang and Clandinin,  
47 2018). Photoreceptor signals are split into parallel ON and OFF pathways in the lamina and  
48 medulla (Behnia et al., 2014; Clark et al., 2011; Joesch et al., 2010; Strother et al., 2014), that are  
49 not direction-selective. These signals provide input to T4 and T5 cells, which compute direction-  
50 selective responses along four directions for every point in the fly visual field (Bausenwein et al.,  
51 1992; Henning et al., 2022; Maisak et al., 2013; Shinomiya et al., 2019; Takemura et al., 2013).  
52 The outputs of T4 and T5 cells are then summed across visual space by lobula plate tangential  
53 cells (LPTCs) (Barnhart et al., 2018; Joesch et al., 2008; Maisak *et al.*, 2013; Mauss et al., 2015;  
54 Schnell et al., 2012). Different LPTCs provide distinct signals about the overall pattern of motion  
55 surrounding the fly, and have been linked to head and body movements (Haikala et al., 2013;  
56 Kim et al., 2017; Krapp and Hengstenberg, 1996).

57 Interestingly, there have been several reports of flies turning in the direction opposite to what  
58 would be predicted from the optomotor turning response. In some cases, these counter-intuitive  
59 behaviors were observed using periodic stimuli with spatial wavelengths smaller than the  
60 receptive field of individual ommatidia, and thus can be accounted for by aliasing (Buchner,  
61 1976; Götz, 1964; Götz, 1970). Work in a tethered flight simulator showed that when a moving  
62 pattern is presented in front of the fly, the animal turned in the direction of the stimulus motion  
63 (Tammero et al., 2004), as expected (Goetz, 1968). However, if the moving pattern was  
64 presented behind the fly, it attempted to turn in the direction opposite to stimulus motion  
65 (Tammero *et al.*, 2004). In a different experimental preparation, rotational patterns were  
66 presented on a dome around freely-walking flies (Williamson et al., 2018). Under these  
67 conditions, flies generally turned in the direction of motion of the stimulus, but these rotations  
68 were often punctuated by brief, large-magnitude saccades in the opposite direction. Similarly,  
69 experiments using flight simulators have reported spikes in the torque in the direction opposite  
70 the stimulus rotation (Wolf and Heisenberg, 1990).

71 Here we show that rotational stimuli can elicit strong, consistent anti-directional behavior in two  
72 drosophilid species, *D. melanogaster* and *D. yakuba*. We report that flies respond to high  
73 contrast, high luminance rotational motion stimuli by first turning in the direction of stimulus  
74 motion, and then reversing their trajectory after approximately one second, depending on the  
75 species. In *Drosophila melanogaster*, we characterize the dynamics of this behavior and the  
76 stimuli that drive it. The behavior depends critically on adaptation to back-to-front motion. We

77 use the genetic tools available in *Drosophila melanogaster* to show that this behavior relies on  
78 the motion detecting neurons T4 and T5. Silencing HS and CH, two widefield neurons  
79 downstream of T4 and T5, resulted in small changes in this complex turning behavior. However,  
80 the visually evoked responses of these direction-selective neurons could not account for these  
81 behaviors. Thus, behavioral reversal must be mediated by more downstream circuitry. Overall,  
82 these results show that flies generate behavioral signals that oppose the direction of visual  
83 motion, showing that *Drosophila* turning responses to wide-field visual motion stimuli are more  
84 complex than a simple stabilizing reflex.

## 85 **Results**

### 86 **Anti-directional turning responses to high contrast stimuli**

87 Optomotor turning responses are central for gaze stabilization, so we sought to examine the  
88 stability of this response across different conditions. Many studies have investigated this  
89 behavior using low contrast and low light intensity stimuli or both (Bahl et al., 2013; Bosch et  
90 al., 2015; Buchner, 1976; Götz and Wenking, 1973; Rister et al., 2007; Seelig et al., 2010), at a  
91 variety of different speeds. However, natural scenes can have relatively high contrast and  
92 luminance, conditions have been poorly explored in the laboratory. In this experiment, we  
93 presented flies with rotational stimuli using high contrast and relatively high luminance.

94 We tethered individual female *D. melanogaster* above a freely rotating ball to characterize the  
95 optomotor response (Buchner, 1976; Creamer et al., 2019) (**Fig. 1a**). As expected, low contrast,  
96 slow-moving sinusoidal gratings caused flies to turn in the same direction as the moving gratings  
97 via the classical optomotor turning response (**Fig. 1b**) (Bahl et al., 2013; Bahl et al., 2015;  
98 Buchner, 1976; Clark et al., 2011; Clark et al., 2014; Creamer et al., 2018; Götz, 1964;  
99 Hassenstein and Reichardt, 1956; Leonhardt et al., 2016; Salazar-Gatzimas et al., 2016; Seelig et  
100 al., 2010; Silies et al., 2013; Strother et al., 2018; Strother et al., 2017; Tammero et al., 2004).  
101 However, when we changed the stimulus to high contrast sinusoidal gratings (nominal 100%  
102 Weber contrast), flies turned in the stimulus direction for approximately 1 second, but then  
103 reversed course, and turned in the direction opposite to the stimulus motion for the duration of  
104 the stimulus presentation. Because this turning response is in the opposite direction of stimulus  
105 and the syn-directional optomotor turning response, we refer to it as anti-directional turning.

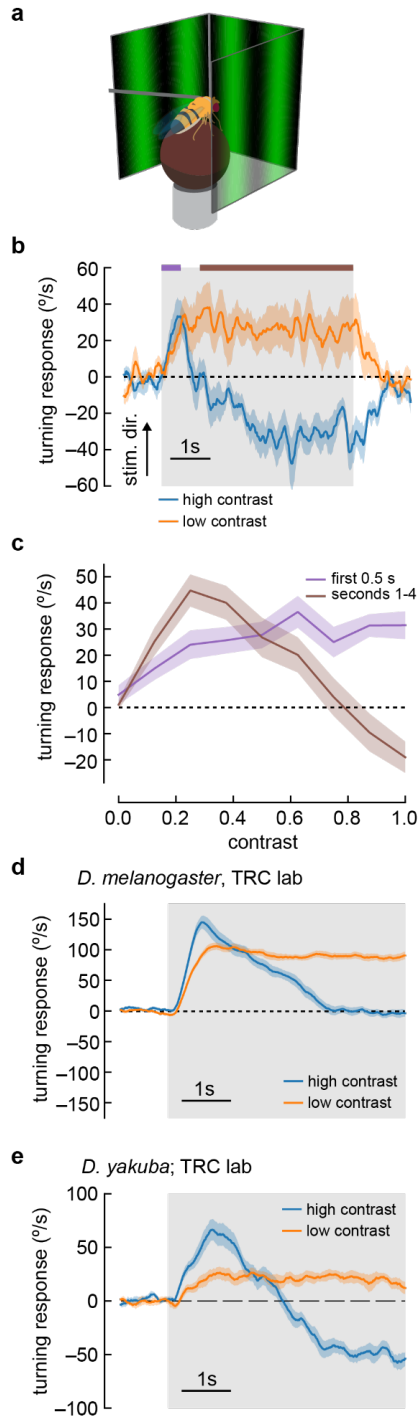
106 We swept a range of contrasts and compared the fly turning in the first 500 milliseconds to the  
107 turning after one second (**Fig. 1c**). As contrast increased, the flies turned faster during the first  
108 half second of stimulus presentation, reaching a plateau at around 0.5 contrast, consistent with  
109 previous results (Bahl et al., 2015; Buchner, 1976; Duistermars et al., 2007; Heisenberg and  
110 Buchner, 1977; McCann and MacGinitie, 1965; Strother et al., 2017). Fly behavior after the first  
111 second of stimulation was more complex. As contrast increased from 0 to 0.25, flies turned in the  
112 same direction as the stimulus, with faster turning as the contrast increased. When the contrast  
113 was greater than 0.25, turning decreased, lowering to no net sustained turning at around 0.8  
114 contrast. Above a contrast of 0.8, flies began to turn in the direction opposite the stimulus.

115 These initial experiments took place in the lab of author DAC. To confirm that these unexpected  
116 responses did not reflect some idiosyncrasy of one specific behavioral apparatus or environment,  
117 we repeated these experiments in a second lab, that of author TRC. Under similar conditions,

118 using the same strain of *Drosophila melanogaster*, we reproduced the rapid deceleration after an  
119 initial, transient syn-directional response (**Fig. 1d**), with some individual flies exhibiting  
120 significant anti-directional turning, as in the experiments in the first lab (**Supp. Fig. S1**). This  
121 demonstrates that the key features of this behavioral response are stable across experimental  
122 systems and laboratories, though the magnitude of reverse-turning behavior in *D. melanogaster*  
123 is sensitive to some unknown experimental parameter differences between the laboratories.

124 Individual strains of *D. melanogaster*, and other drosophilid species, display significant variation  
125 in their locomotor patterns during walking (York et al., 2022). Indeed, when we tested a Canton-  
126 S *D. melanogaster* strain, we observed mild but significant anti-directional turning at long  
127 timescales (**Supp. Fig. S2b**). We reasoned that a strong test of the generality of anti-directional  
128 turning would be to examine turning behavior in another species, and selected *D. yakuba*.  
129 Strikingly, *D. yakuba* also displayed anti-directional turning behavior under similar conditions  
130 (**Fig. 1e**). Thus, this behavior is not an idiosyncratic feature of a single laboratory strain.

131



132

133 **Figure 1. Flies turn opposite to the stimulus direction in high contrast conditions**

134 a) We measured fly turning behavior as they walked on an air-suspended ball. Stimuli were  
135 presented over 270 degrees around the fly.

136 b) We presented drifting sinusoidal gratings for 5 seconds (shaded region) with either high  
137 contrast ( $c = 1.0$ ) or low contrast ( $c = 0.25$ ). When high contrast sinusoidal gratings were  
138 presented, flies initially turned in the same direction as the stimulus, then started turning

- 139 in the opposite direction after ~1 second of stimulation. Under low contrast conditions,  
140 flies turned continuously in the same direction as the stimulus. In these experiments, the  
141 sine waves had a wavelength of 60° and a temporal frequency of 1 Hz. Shaded patches  
142 represent  $\pm 1$  SEM. N = 10 flies.
- 143 **c)** We swept contrast between 0 and 1 and measured the mean turning response during the  
144 first 0.5 seconds (purple, purple bar in **b**) and during the last 4 seconds of the stimulus  
145 (brown, brown line in **b**). The response in the first 0.5 seconds increased with increasing  
146 contrast, while the response in the last four seconds increased from  $c = 0$  to  $c = 0.25$ , and  
147 then decreased with increasing contrast, until flies turned in the direction opposite the  
148 stimulus direction at the highest contrasts. N = 20 flies.
- 149 **d)** We repeated the presentation of drifting sinusoidal gratings, this time in the lab of author  
150 TRC, using a similar behavioral apparatus. Stimulus parameters were as described in (b).  
151 In these experiments, the population average shows that flies proceeded to zero net  
152 turning at high contrasts, but some individual flies exhibited anti-directional turning  
153 responses. N = 20 flies.
- 154 **e)** We repeated the experiments with *D. yakuba*, also in the lab of TRC, and observed that  
155 this species exhibited a robust anti-directional turning response to high contrast gratings  
156 and a classical syn-directional turning response to low contrast gratings. N = 11 flies.

157

### 158 **Conditions for anti-directional turning behaviors**

159 While anti-directional turning behaviors have been reported before, other groups have presented  
160 similar stimuli without observing anti-directional behavior (Bahl *et al.*, 2013; Bosch *et al.*, 2015;  
161 Buchner, 1976; Götz and Wenking, 1973; Seelig *et al.*, 2010). We wondered what aspects of our  
162 experimental setup could lead to these behavioral differences. In our experiments, anti-  
163 directional turning was strongly linked to display brightness (**Supp. Fig. S2a**). When the mean  
164 brightness of the screens was reduced from 100 cd/m<sup>2</sup> to 1 cd/m<sup>2</sup>, we saw no anti-directional  
165 turning in 5 second trials (though average optomotor behavior did decrease over the course of the  
166 stimulus presentation). When we further reduced the mean brightness to 0.1 cd/m<sup>2</sup>, flies persisted  
167 in their optomotor behavior throughout the stimulus presentation. We note, however, that at low  
168 luminance, low levels of ambient light in the nominally dark experimental rig could also reduce  
169 the effective contrast of the stimulus.

170 We tested a variety of other factors that might affect anti-directional turning. Anti-directional  
171 turning occurred when experiments were run both at hot temperatures and at room temperature  
172 (**Supp. Fig. S2b**). We also observed anti-directional behavior when flies were reared in the dark  
173 and on different media. We also tested a number of other experiment conditions (**Supp. Fig.**  
174 **S2c**). Flies responded with anti-directional turning to high contrast stimuli presented at both blue  
175 and green wavelengths. We glued fly heads to their thorax to ensure stimuli could not be affected  
176 by head movements (Haikala *et al.*, 2013; Kim *et al.*, 2017), but found no difference between  
177 head-fixed and head-free flies. There were, however, a few factors that did modulate anti-  
178 directional turning behavior. In particular, rearing *D. melanogaster* at 25°C instead of 20°C or  
179 testing flies that were two weeks old instead of 12-60 hours old both reduced overall turning

180 behavior and eliminated anti-directional turning. In these cases, optomotor turning still decreased  
181 over the course of the 5 second, high contrast trials, but did not reverse. As details of rearing  
182 temperature and the age at which behavior tests are run often vary across labs, it is likely that  
183 these factors account for the differences between our observations and the previous literature.

184

### 185 [Distinct spatiotemporal tuning of the anti-directional behavioral response](#)

186 To further characterize the anti-directional response, we swept the spatial and temporal  
187 frequency of the sinusoidal grating stimulus. Using only Weber contrasts of 1, we compared the  
188 early response (first quarter second, **Fig. 2a**) to the late response (after one second, **Fig. 2b**).  
189 *Drosophila melanogaster* always turned in the optomotor direction during the early stimulus  
190 response. In this early response, flies turned most vigorously to stimuli with short spatial  
191 frequencies ( $\sim 20^\circ$  wavelength) and fast temporal frequencies ( $\sim 8$  Hz), in agreement with earlier  
192 studies (Creamer *et al.*, 2018; Strother *et al.*, 2018; Tammero *et al.*, 2004). However, during the  
193 long-term response to high-contrast stimuli, flies only turned in the optomotor direction at very  
194 high temporal frequencies ( $> \sim 16$  Hz) and at very low temporal frequencies ( $< 0.5$  Hz). At  
195 intermediate temporal frequencies, flies showed a sustained anti-directional response. The  
196 maximal anti-directional response was achieved at 1 Hz and  $45^\circ$  wavelength, distinct from the  
197 conditions for peak classical turning responses. Interestingly, the stimuli that elicit the strongest  
198 anti-directional response appear similar to those that maximally activate T4 and T5 neurons  
199 when those neurons are measured in head-fixed flies (Arenz *et al.*, 2017; Creamer *et al.*, 2018;  
200 Leong *et al.*, 2016; Maisak *et al.*, 2013; Strother *et al.*, 2018; Wienecke *et al.*, 2018).

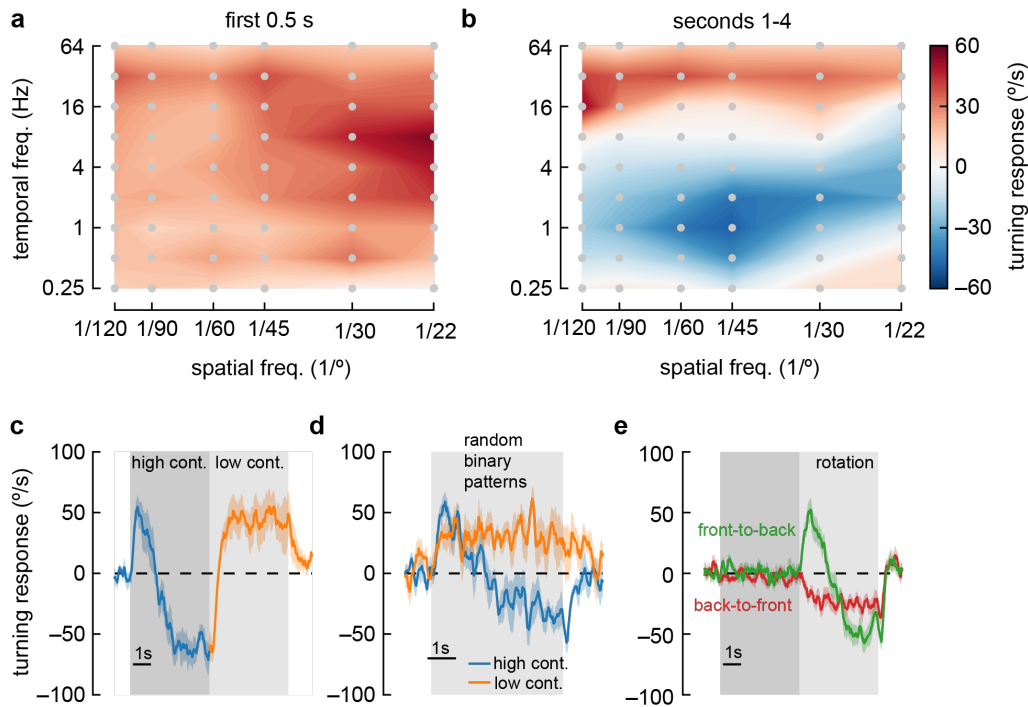
201

### 202 [Anti-directional turning results from adaptation effects](#)

203 We were intrigued by the switch from syn-directional to anti-directional turning behavior. To  
204 investigate the dynamics of these changes, we presented a rotating sinusoidal stimulus at contrast  
205 1 for five seconds, and then changed the contrast to 0.25 (**Fig. 2c**). After the switch to low  
206 contrast, the flies quickly reverted classical, syn-directional optomotor behavior, demonstrating  
207 that no long-term switch in directional turning occurs during high contrast stimulus presentation.  
208 This effect did not depend on the periodic nature of these stimuli; a rotating stimulus consisting  
209 of  $5^\circ$ -wide vertical bars with randomly-chosen, binary contrasts (Clark *et al.*, 2014) yielded  
210 similar behavioral responses (**Fig. 2d**).

211 To further isolate the causes of this switch in behavior, we developed a stimulus to adapt the fly  
212 to different stimuli before presenting high-contrast rotational sinusoidal gratings to elicit the anti-  
213 directional turning response. This adapting stimulus consisted of five seconds of high contrast  
214 ‘translational’ stimuli, which was then followed by a rotational stimulus (**Fig. 2e**). The  
215 translational stimuli consisted of both left and right hemifields moving either front-to-back or  
216 back-to-front across the fly’s two eyes (Creamer *et al.*, 2018). These stimuli resulted in no net  
217 turning by the flies (Creamer *et al.*, 2018; Silies *et al.*, 2013). Adapting the fly with front-to-back  
218 stimuli did not have a strong effect on the subsequent response to rotational stimuli. However,  
219 adapting with back-to-front stimuli generated responses that no longer showed an initial syn-

220 directional turning response, but instead exhibited anti-directional turning immediately after the  
 221 rotational stimulus began. This result indicates that the anti-directional turning results from slow-  
 222 timescale changes that depend on strong back-to-front motion stimulation.



223

224 **Figure 2. Anti-directional turning behavior has distinct tuning and is driven by adaptation.**

- 225 **a)** Heatmap of fly turning velocity during the first 0.5 seconds of sinusoidal grating  
 226 stimulation under high contrast conditions and variable temporal and spatial frequencies.  
 227 The flies turned in the direction of the stimulus across all conditions and responded most  
 228 to 8 Hz, 22-degree stimuli. N = 16,21,17,21,7, and 22 flies for spatial frequencies 1/120,  
 229 1/90, 1/60, 1/45, 1/30 and 1/22 degrees respectively.
- 230 **b)** Heatmap as in (a), measured during the last four seconds of stimulation. Flies turned in  
 231 the same direction as the stimulus at high and low temporal frequencies, but in the  
 232 opposite direction of the stimulus at intermediate temporal frequencies, with a maximal  
 233 anti-directional response at wavelengths between 30° and 60°.
- 234 **c)** Switching stimulus contrast from high to low after 5 seconds caused flies to revert to syn-  
 235 n-directional behavior after the anti-directional response. N = 7 flies.
- 236 **d)** Presenting rotating random binary patterns (5-degree vertical strips rotating at 150  
 237 degrees/second) induced anti-directional turning similar to that elicited by rotating sine  
 238 wave gratings. N = 7 flies.
- 239 **e)** We presented flies with five seconds of “translational” stimuli (dark shaded region), with  
 240 high contrast sinusoidal gratings moving either front-to-back or back-to-front, bilaterally,  
 241 for five seconds. After that, we presented high contrast rotational sinusoidal grating  
 242 stimuli (60° wavelength, 1 Hz). Front-to-back stimulation did not affect the subsequent  
 243 response to rotational stimuli, but back-to-front stimuli caused flies to turn immediately  
 244 in the opposite direction of the stimulus. N = 18 flies.



245

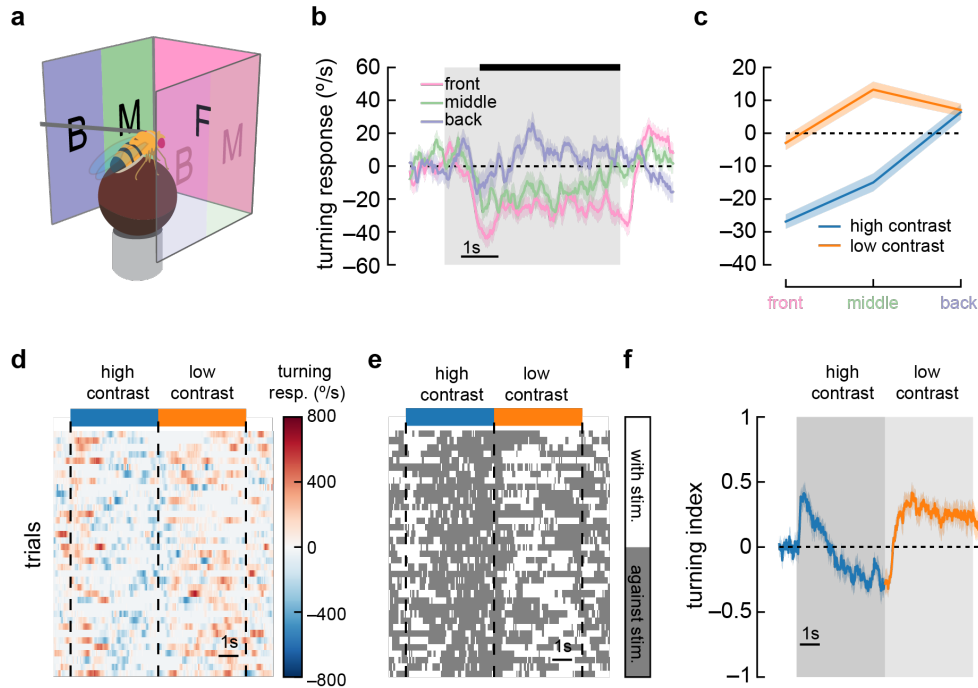
### 246 Anti-directional turning is elicited when stimuli are presented in front of the fly

247 A previous report of anti-directional turning behavior in flying tethered flies showed that flies  
248 turn in the opposite direction to stimuli that are presented behind their midline (Tammero *et al.*,  
249 2004). To test whether our results were caused by this effect, we split our stimulus into three  
250 regions: 90 degrees in front of the fly, 45 degrees in front of the midline on either side of the fly,  
251 and 45 degrees behind the midline on either side of the fly (**Fig. 3a**). We found that flies  
252 displayed anti-directional turning when presented with stimuli only in the front region or only  
253 just in front of the midline (**Fig. 3bc**). They did not display anti-directional turning when moving  
254 stimuli were presented behind the midline (**Fig. 3bc**). This suggests a different mechanism from  
255 the behaviors that depend on posterior spatial location to elicit reverse-turning (Tammero *et al.*,  
256 2004).

257

### 258 Anti-directional responses do not depend on saccades

259 Anti-directional saccades have been reported in walking and flying flies (Williamson *et al.*,  
260 2018; Wolf and Heisenberg, 1990). In walking flies (Williamson *et al.*, 2018), flies largely  
261 turned in syn-directionally, but these turns were sometimes interrupted by brief, high-amplitude  
262 saccades in the opposite direction, against the stimulus direction. If such saccades were frequent  
263 or high amplitude, the net effect could shift the average turning we measured, creating apparent  
264 anti-directional turning. To investigate this possibility, we plotted the turning response on a per-  
265 trial basis (**Fig. 3d**). We then discarded information about the magnitude of the turns and  
266 considered only the direction of the turning at each point in time (**Fig. 3e**). Strikingly, in many  
267 trials, flies continued to turn opposite to the stimulus for several seconds, a behavior unlike brief  
268 saccades. We then calculated a turning index for each response timepoint (sampled at 60 Hz).  
269 This turning index represented the fraction of trials where the fly turned in the direction of the  
270 stimulus at each timepoint minus the fraction of trials where the fly turned in the opposite  
271 direction (**Fig. 3f**). Since this turning index does not include the magnitude of turning, it is  
272 strongly affected by sustained low-amplitude turns and discounts any brief high-amplitude  
273 saccades. When presented with high contrast stimuli, flies maintained a negative turning index,  
274 indicating that sustained turns, and not high velocity saccades, underlie this anti-directional  
275 turning behavior.



276

277 **Figure 3. Anti-directional turning is driven by stimuli in the forward-facing visual field and**  
 278 **is not driven by saccades.**

- 279 **a)** We divided our panoramic display into three sections — the front 90°, the 45° behind the  
 280 fly on either side, and a middle 45°.
- 281 **b)** High contrast sinusoidal gratings were presented on each of these three display sections,  
 282 with the remaining sections blank. Flies turned syn-directionally when stimuli were  
 283 presented behind the fly, and turned anti-directionally when stimuli were presented in  
 284 front of the fly. Shaded patches represent  $\pm 1$  SEM.  $N = 55$  flies.
- 285 **c)** Average turning in the last 4 seconds of the stimulus (black bar in **b**), in low contrast and  
 286 high contrast conditions. Shaded patches in the time trace plots represent  $\pm 1$  SEM.  $N =$   
 287 55 flies.
- 288 **d)** A single fly responds to many trials of sinusoidal grating stimuli at high contrast (blue  
 289 bar) and low contrast (orange bar). We show a heatmap of the fly's responses over time  
 290 (horizontal axis) and across trials (vertical axis).
- 291 **e)** We can ignore the magnitude of the turning and instead only quantify whether the fly was  
 292 turning in the same direction as the stimulus (white area) or in the opposite direction  
 293 (dark gray area). This shows sustained anti-directional turning, not brief saccades.
- 294 **f)** Averaging the direction (but not magnitude) of turning across trials and across flies  
 295 yields a turning index for each point in time. Shaded patches in the time trace plots represent  $\pm 1$   
 296 SEM.  $N = 7$  flies.

297 [Anti-directional turning requires elementary motion detectors](#)

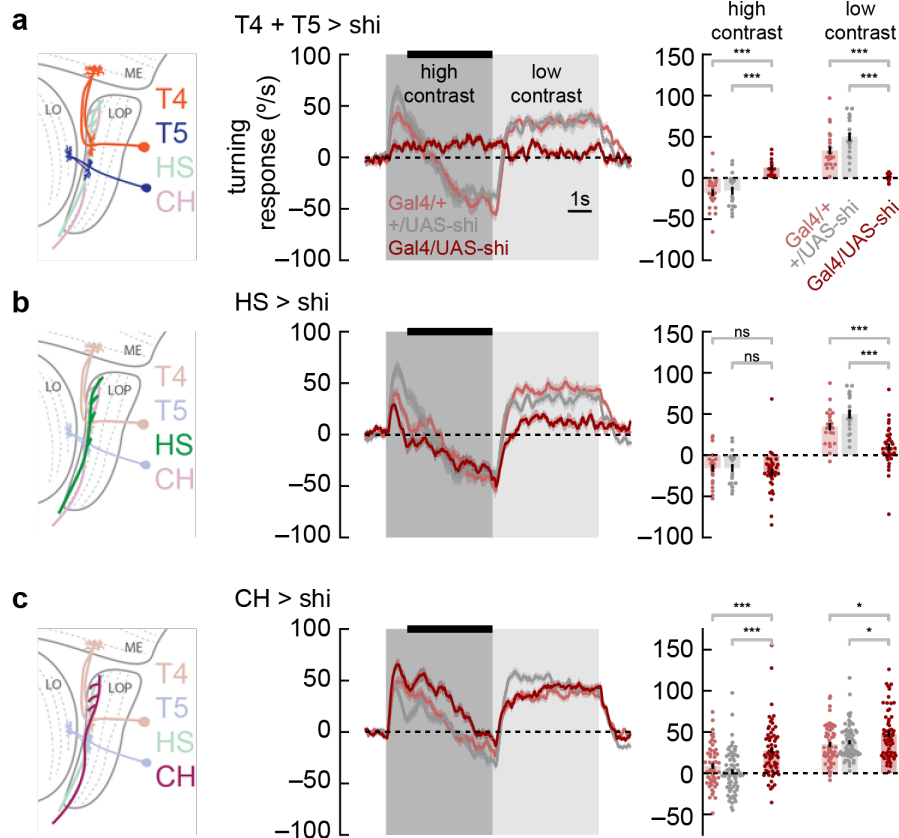
298 What neurons are involved in this anti-directional turning behavior? Previous work demonstrated  
 299 that T4 and T5 are required for directional neural responses (Schnell *et al.*, 2012), as well as for  
 300 optomotor turning (Maisak *et al.*, 2013; Salazar-Gatzimas *et al.*, 2018; Salazar-Gatzimas *et al.*,

301 2016), for walking speed regulation (Creamer *et al.*, 2018), and for responses to visual looming  
302 stimuli (Schilling and Borst, 2015). We silenced the neurons T4 and T5 using *shibire<sup>ts</sup>*  
303 (Kitamoto, 2001) and measured responses to sinusoidal stimuli that switched from high to low  
304 contrast (**Fig. 4a**). Flies in which T4 and T5 had been silenced displayed only minimal responses  
305 to motion stimuli, with anti-directional turning suppressed along with classical syn-directional  
306 turning. Thus, we conclude that, like optomotor turning behaviors, this anti-directional behavior  
307 depends critically on signals from T4 and T5.

#### 308 **Anti-directional turning requires the CH lobula plate tangential cell**

309 Since the switch from optomotor to anti-directional behavior seems to be dependent on the  
310 direction of motion adaptation (**Fig. 2e**), we reasoned that neurons involved in this behavior were  
311 likely to be downstream from T4 and T5. Horizontal System (HS) cells are well-studied  
312 postsynaptic partners of T4 and T5 (Joesch *et al.*, 2008; Joesch *et al.*, 2010). These lobula plate  
313 tangential cells integrate information from front-to-back and back-to-front selective T4 and T5  
314 cells across the fly's visual field (Mauss *et al.*, 2015). HS cells have been implicated in visually-  
315 evoked head turns (Kim *et al.*, 2017) and body rotations in flight (Haikala *et al.*, 2013), as well  
316 as in maintenance of walking direction (Fujiwara *et al.*, 2022). When we silenced HS neurons,  
317 we found small deficits in syn-directional turning behavior, but not in anti-directional turning  
318 behavior (**Fig. 4b**), indicating that HS cells synaptic output is not required specifically for anti-  
319 directional turning behavior.

320 Next, we turned to the CH lobula plate tangential cells. These cells are GABAergic and are both  
321 pre-synaptic and post-synaptic in the lobula plate (Wei *et al.*, 2020). In blowflies, these neurons  
322 play an inhibitory role in an interconnected LPTC circuit that shapes behavior (Borst and Weber,  
323 2011). When we silenced these neurons, we found a small increase in syn-directional turning and  
324 a decrease in anti-directional turning (**Fig. 4c**). Overall, silencing this neuron type caused the  
325 flies to turn more in the direction of motion. This result suggests that CH activity contributes to  
326 the anti-directional turning response. However, since adapting to back-to-front translational  
327 stimuli significantly affected the dynamics of anti-directional turning, it seems likely that other  
328 neurons beyond HS and CH are involved, since these two neurons both respond selectively to  
329 front-to-back motion (Eckert and Dvorak, 1983; Joesch *et al.*, 2008).



330

331 **Figure 4. Syn-directional and anti-directional turning share common circuitry**

- 332 **a)** We silenced T4 and T5 neurons by expressing *shibire<sup>ts</sup>* selectively in those neurons. We  
 333 measured turning behavior during a contrast-switching stimulus (as in **Fig. 2c**). Results  
 334 from flies with T4 and T5 silenced shown in dark red, while controls are in light red and  
 335 gray. Average fly behavior during the last four seconds of the first contrast (black bar on  
 336 left) shown as bars on the right, with individual fly behavior shown as dots. Note that the  
 337 data labeled “low contrast” are from experiments in which the low-contrast stimulus was  
 338 shown before the high contrast stimulus. Shaded patches in the time trace plots represent  
 339  $\pm 1$  SEM, as do vertical lines on bar plots. \*\*\* indicates experimental results are  
 340 significantly different from results,  $P < 0.001$  via a two-sample Student t-test. \* indicates  
 341  $P < 0.05$ . N = 17, 24, 19 flies with genotypes T4T5/*Shibire<sup>ts</sup>*, T4T5/+, +/*Shibire<sup>ts</sup>*.  
 342 **b)** Results from HS silencing as in **a**. Silencing HS reduced syn-directional turning behavior  
 343 ( $P < 0.001$ ) but did not have a strong effect on anti-directional turning. N = 34, 21, 19  
 344 flies with genotypes HS/*Shibire<sup>ts</sup>*, HS/+, +/*Shibire<sup>ts</sup>*.  
 345 **c)** Results from CH silencing as in **a**. CH silencing reduced the degree of anti-directional  
 346 turning ( $P < 0.001$ ). N = 63, 57, 70 flies with genotypes CH/*Shibire<sup>ts</sup>*, CH/+, +/*Shibire<sup>ts</sup>*.

347

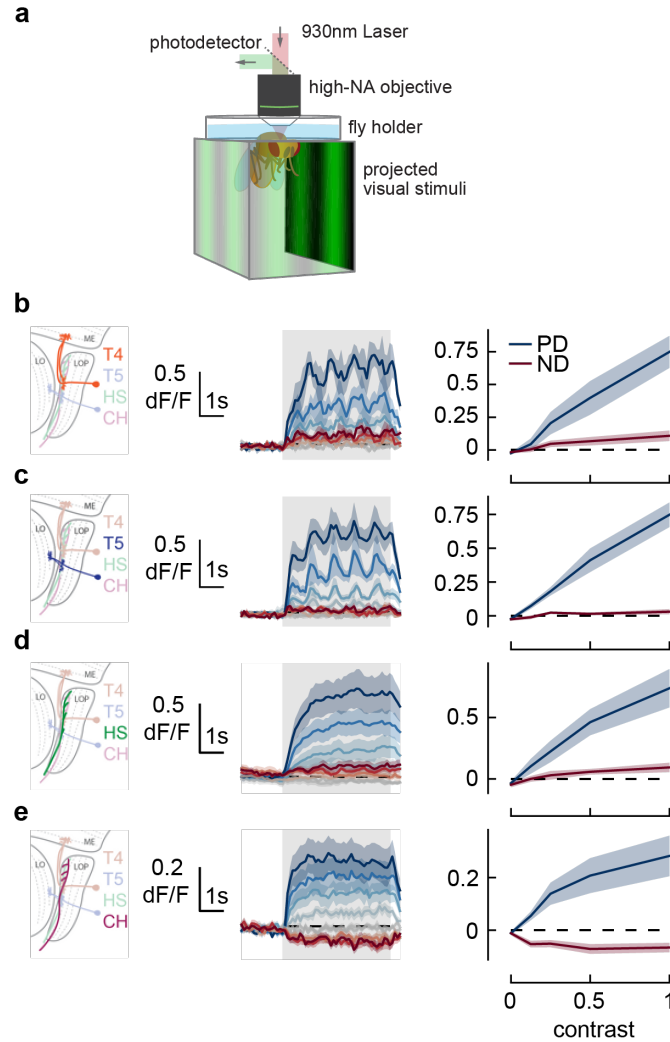
348 **Early direction-selective cells do not adapt to the stimulus**

349 The anti-directional turning response is preceded by an initial syn-directional response. This  
 350 change in behavior must be the result of changes in neural activity, but this change could happen

351 at any point along the neural pathway between photoreceptors and motor neurons. In order to  
352 constrain possible mechanisms for generating the anti-directional turning behaviors, we used  
353 calcium imaging to interrogate the activity of direction selective neurons during high and low  
354 contrast stimulation (**Fig. 5a**). However, as calcium imaging experiments using two photon  
355 microscopy require additional spectral filtering of the projector, we first confirmed that these  
356 spectral differences did not alter anti-directional turning responses. To do this, we re-measuring  
357 the anti-directional turning behavior using optical filtering matched to the conditions needed for  
358 imaging. Using this spectrally distinct illuminant, we observed both syn-directional and anti-  
359 directional turning behaviors, following the previously observed dynamics (**Supp. Fig. S3**).

360 As T4 and T5 neurons play a critical role in both the syn- and anti-directional turning responses,  
361 we first measured the calcium activity of these neurons as they responded to sine wave gratings  
362 at a range of contrasts in their preferred and null directions. The T4 and T5 neurons responded to  
363 sine wave gratings in their preferred direction by increasing their calcium activity for the full  
364 duration of the stimulus presentation, reaching a plateau after approximately 1 second (**Fig. 5bc**,  
365 middle). As we increased the contrast of the preferred direction stimuli, we found that both T4  
366 and T5 cells had increased calcium activity throughout the contrast range (**Fig. 5bc**, right),  
367 consistent with prior measurements (Maisak *et al.*, 2013). Thus, the responses of T4 and T5 cells  
368 do not capture the transition from syn-directional to anti-directional turning behavior.

369 Next we examined two LPTCs downstream of T4 and T5 cells. Calcium activity in HS cells  
370 followed similar trends to T4 and T5. Calcium signals increased at the start of preferred direction  
371 stimuli presentation and stayed high until the end of the presentation (**Fig. 5d**, middle).  
372 Increasing contrast caused stronger calcium responses with a mild saturation effect at high  
373 contrast (**Fig. 5d**, right), consistent with prior voltage measurements (Joesch *et al.*, 2008). These  
374 results indicate that the changes in the time course of optomotor behavior at high contrast are not  
375 related to changes in HS activity. Finally, we measured calcium activity in CH cells. CH cells  
376 responded to visual stimuli more quickly than HS cells (**Fig. 5e**, middle), and showed decreased  
377 calcium signals in response to null direction stimuli (**Fig. 5e**, right). However, they showed  
378 sustained responses to high contrast stimuli, as in T4, T5, and HS. These measurements suggest  
379 that the switch from syn- to anti-directional turning behavior is driven by cells downstream of or  
380 parallel to T4, T5, HS, and CH.



381

382 **Figure 5. Responses in early direction-selective cells do not show a reduction or reversal of**  
383 **response on the timescale of the behavior.**

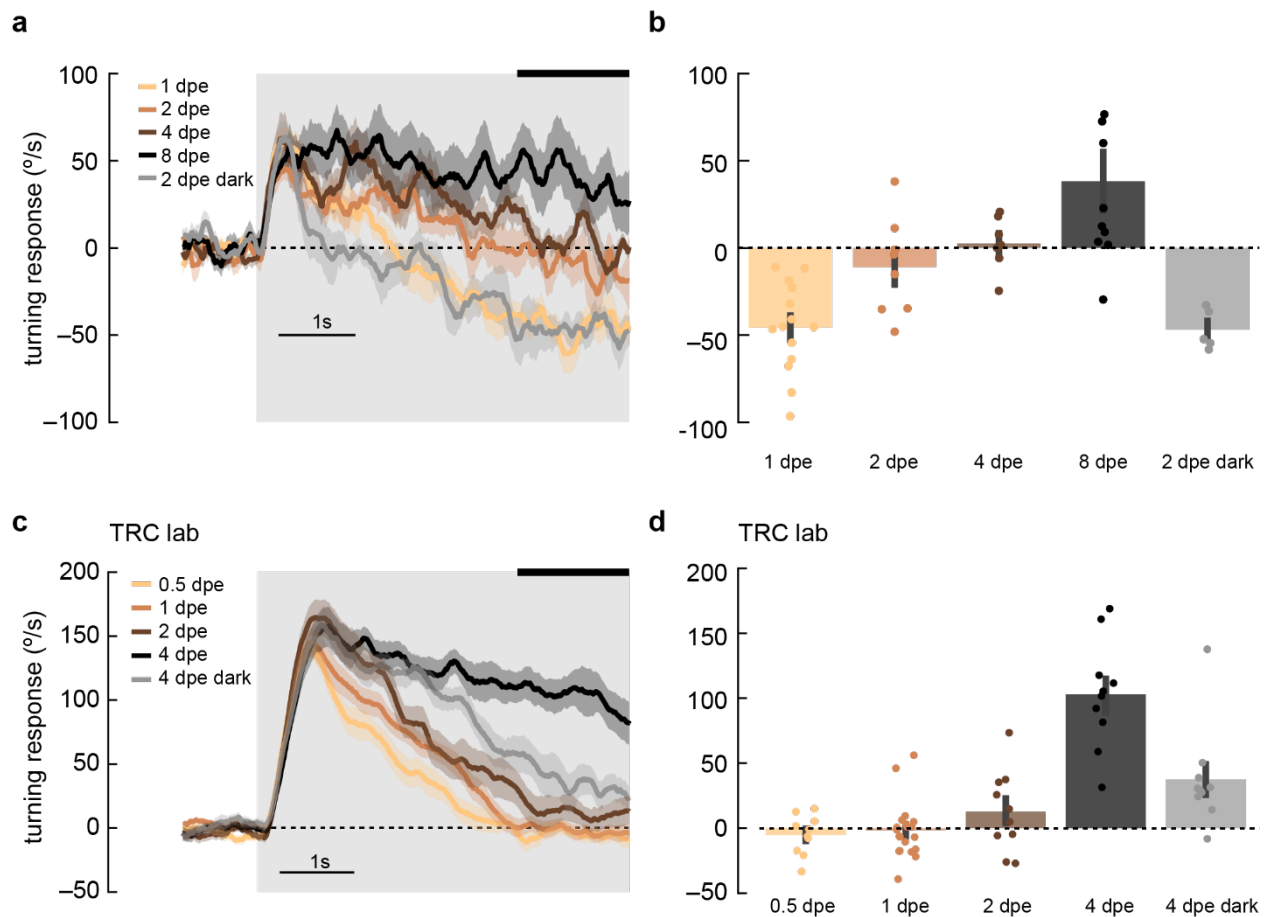
- 384 a) We used two-photon microscopy to measure calcium activity in lobula plate neurons  
385 while presenting sinusoidal gratings at a range of contrasts.  
386 b) T4 cells, marked in orange (*left*), responded to drifting sinusoidal gratings with increased  
387 calcium activity (*middle*). Darker colors indicate higher contrast, preferred direction in  
388 blue, null direction in red. When integrated across the stimulus presentation (*right*),  
389 calcium activity increased with stimulus contrast. N = 8 flies.  
390 c-e) As in b) measuring calcium activity in T5, HS, and CH cells. N = 8, 10, 15 flies.

391

### 392 **Adult plasticity in anti-directional turning behavior**

393 In behaving flies, the strength of anti-directional turning was dependent both on rearing  
394 temperature, which alters the rate of growth, and on age (**Supp. Fig. S2**). This raises the  
395 possibility that syn- and anti-directional turning responses might be plastic during the early adult  
396 stages of development. To probe this possibility, we presented 1 Hz, high-contrast, rotating

397 sinusoidal grating at various stages during early adulthood (**Fig. 6**). Strikingly, as flies aged from  
398 0.5 to 4 days post eclosion (dpe), the initial syn-directional turning became less transient and  
399 more sustained, indicative of a weaker anti-directional turning drive. We then wondered whether  
400 this plasticity was intrinsically programmed, or dependent on visual input. To explore this  
401 possibility, we reared flies in darkness to 2 or 4 dpe and measured their turning responses (**Fig. 6**,  
402 *gray*). Dark-reared flies exhibited a stronger deceleration away from syn-directional turning,  
403 similar to that found in more juvenile flies, arguing that visual input may sculpt the balance of  
404 syn- and anti-directional turning. Finally, we examined whether optomotor response plasticity  
405 could be detected in *D. yakuba*. However, in this species, anti-directional responses were stable  
406 across the first four days of adulthood, arguing that the role of visual experience in shaping these  
407 responses is itself evolutionarily tuned in drosophilids (**Supp. Fig. 4**).  
408



409

#### 410 **Figure 6. Maturation of optomotor response in early adulthood**

411 a) Adult flies at various ages post eclosion were presented with 5-second, high-contrast,  
412 rotating sinusoidal gratings as in **Fig 2b**. As the flies aged from 1 day post eclosion (dpe)  
413 to 2, 4, and 8 dpe, the initial anti-directional turning response transitioned into syn-  
414 directional turning. Dark-rearing flies at 2 dpe reduced this maturation effect. Shaded  
415 patches represent  $\pm 1$  SEM. N = 5-14 flies.

- 416       **b)** The last 1.5 seconds of the mean turning velocity of each fly was averaged, and the  
417            population response was plotted.
- 418       **c)** As in (a) but in the TRC lab, using 0.5, 1, 2, and 4 dpe, with dark rearing for 4 dpe. With  
419            maturation, the syn-directional turning became less transient. N = 9-15 flies.
- 420       **d)** As in (b) but for data in (c).

421

## 422 **Discussion**

423 In this study, we found we could elicit robust turning in the opposite direction of high contrast  
424 motion stimuli (**Fig. 1**). This behavior is qualitatively different from other turning behaviors  
425 reported in the literature (**Figs. 2 and 3**), but shares elements with the circuitry necessary for  
426 optomotor behavior (**Fig. 4**). However, the switch from optomotor behavior to anti-directional  
427 turning behavior is not a reflection of changes in the activity of known direction-selective neuron  
428 types in the early visual system (**Fig. 5**). Moreover, this anti-directional turning behavior exhibits  
429 a degree of experience-dependent plasticity (**Fig. 6**).

### 430 **Anti-directional turning is distinct from other against-stimuli behaviors**

431 The anti-directional turning behavior we have characterized is distinct from previous reports of  
432 flies turning in the direction opposite to the stimulus motion. First, some opposite-direction  
433 turning behaviors can be explained by stimulus aliasing (Buchner, 1976). Aliasing cannot  
434 explain our results because the stimulus that maximally activates anti-directional behavior has a  
435 spatial frequency of 1/60 cycles per degree, well below the Nyquist frequency of the fly eye  
436 (~1/10 cycles per degree) (Buchner, 1976; Götz, 1970) and below reports of higher acuity vision  
437 in flies (Juusola et al., 2017). Aliasing would also not explain the dependence on stimulus  
438 contrast.

439 Second, our observations also cannot be explained by stimuli to the rear of the fly driving it in  
440 the opposite direction (Tammero *et al.*, 2004), since we observe anti-directional turning even  
441 when stimuli are only presented in only the 90 degrees in front of the fly (**Fig. 3**).

442 Third, it is also distinct from previous reports of reverse body saccades (Williamson *et al.*, 2018)  
443 since it manifests in persistent turns in the opposite direction of the stimulus and can be  
444 measured even when the magnitude of the turns is discarded (**Fig. 3**).

445 Fourth, the behavior observed here also appears to be distinct from previously-observed  
446 stimulus-density dependent behavioral reversals (Katsov and Clandinin, 2008). Those previously  
447 reported behaviors showed immediate reversals, but it took ~1 second for flies in our paradigm  
448 to switch between optomotor and anti-directional behaviors.

### 449 **Anti-directional turning is unlikely to be due to adaptation to contrast alone**

450 In mammalian retina, the direction preference of cells can switch because of upstream circuit  
451 adaptation (Rivlin-Etzion et al., 2012; Vlasits et al., 2014). However, we do not believe the anti-  
452 directional turning we observe has similar causes. In the mammalian retina, direction switching  
453 occurs when non-direction-selective neurons adapt to high contrast stimuli, which distorts the  
454 downstream direction-selective computation. Since the adaptation in those experiments occurs in



455 non-direction-selective neurons, it cannot be affected by the direction of the adapter stimulus.  
456 However, we see differences in turning behavior depending on whether we adapt with front-to-  
457 back or back-to-front stimuli (**Fig. 2e**). This observation rules out a mechanism based solely on  
458 contrast, since the contrast content of front-to-back and back-to-front stimuli are identical.

459 The fly's visual system, however, adapts its gain to stimulus contrast (Drews et al., 2020;  
460 Matulis et al., 2020). Importantly, the phenomenology of the anti-directional turning also argues  
461 that the contrast adaptation is incomplete or heterogeneous among neurons, since contrast 1 and  
462 contrast 0.25 stimuli result in such different behaviors. Contrast adaptation reported in the fly is  
463 also faster than the 1-2 seconds preceding the shift to anti-directional turning in these  
464 experiments.

#### 465 [Anti-directional turning behavior may require specific experimental and rearing conditions](#)

466 Despite these previous reports of anti-directional turning under certain conditions, other labs  
467 have measured sustained optomotor turning in response to high contrast stimuli (Bosch *et al.*,  
468 2015; Götz and Wenking, 1973; Seelig *et al.*, 2010; Strother *et al.*, 2017). We suspect that the  
469 two major causes of this difference are display brightness and rearing temperature. Some  
470 experiments employ displays with mean luminances less than 5 cd/m<sup>2</sup> (Rister *et al.*, 2007; Seelig  
471 *et al.*, 2010; Strother *et al.*, 2017). Our screens, with a mean luminance of 100 cd/m<sup>2</sup>, are  
472 substantially brighter, but not especially bright when compared to natural scenes. In daytime  
473 natural scenes, foliage and the ground have average luminances of 200-500 cd/m<sup>2</sup> and the sky  
474 has an average luminance of around 4000 cd/m<sup>2</sup> (Frazor and Geisler, 2006). We therefore suspect  
475 that as researchers move to using displays that can more accurately depict natural scene  
476 luminances, anti-directional turning behaviors will be encountered more frequently.

477 Rearing conditions also had a significant influence on anti-directional turning behavior. Flies  
478 reared at 25°C showed less anti-directional behavior than those reared at 20°C. We also found  
479 differences based on fly age and fly strain. Our rearing conditions and choice of fly strain have  
480 all been optimized during previous experiments to yield strong optomotor responses. Since anti-  
481 directional behavior at high contrast usually occurs under conditions that yield strong optomotor  
482 turning at low contrast, these optimized conditions may be required to observe anti-directional  
483 behavior. Temperature, in particular, has developmental effects on neural connectivity (Kiral et  
484 al., 2021). Notably, all three of these parameters vary significantly across the field, with prior  
485 studies varying rearing temperatures from 18 to 20 to 25°C (see for instance (Creamer *et al.*,  
486 2018; Juusola *et al.*, 2017; Ketkar et al., 2020; Mongeau and Frye, 2017; Strother *et al.*, 2017)),  
487 ages from 1 day to 10 days (see for instance (Bahl *et al.*, 2013; Silies *et al.*, 2013; Tammero *et*  
488 *al.*, 2004)), and strain between CantonS or OregonR (see for instance (Clark *et al.*, 2011; Rister  
489 *et al.*, 2007)). Thus, we believe that these factors likely account for the fact that this phenomenon  
490 has not previously been reported.

#### 491 [Tuning of anti-directional turning matches tuning of direction selective neurons](#)

492 The study of anti-directional turning behavior may yield clues about the temporal tuning of fly  
493 motion detectors. Optomotor behavior is tuned to visual stimuli in the range of 8-22 Hz (Creamer  
494 *et al.*, 2018; Strother *et al.*, 2018; Tammero *et al.*, 2004; Tuthill et al., 2013), while anti-  
495 directional behavior is tuned to stimuli in the 0.5-4 Hz range (**Fig. 1**). Intriguingly, this slower

496 tuning matches the tuning of T4, T5, and HS neurons, as measured via calcium imaging or  
497 electrophysiology (Chiappe et al., 2010; Creamer *et al.*, 2018; Joesch *et al.*, 2008; Maisak *et al.*,  
498 2013). Previous studies have suggested that the difference in tuning between behavior and  
499 imaging are due to octopamine released during behavior, and not necessarily released during  
500 imaging (Arenz *et al.*, 2017; Chiappe *et al.*, 2010; Strother *et al.*, 2018). In this work, we  
501 demonstrate a motion-related behavior tuned to low frequencies, comparable to those in neural  
502 measurements, during behavior that requires T4 and T5 neurons. Overall, this suggests that T4  
503 and T5 are required for behaviors with very different temporal tuning, which in turn suggests that  
504 the temporal tuning of behavior is not determined solely by T4 and T5 tuning, but by other,  
505 parallel pathways as well.

#### 506 **Anti-directional turning is unlikely to occur in nature**

507 In a natural environment, flies are unlikely to encounter a situation where they see continuous  
508 motion in the same direction for more than 1 second. Measurements of free walking behavior  
509 have shown that the time constant of the autocorrelation of fly turning is around 100 ms  
510 (DeAngelis et al., 2019; Katsov et al., 2017). This means that the anti-directional turning studied  
511 here has likely not been directly subject to evolutionary pressures. However, the fact that we  
512 observed strong anti-directional turning in *D. yakuba* indicates that anti-directional turning is not  
513 an idiosyncratic behavior of *D. melanogaster*. It seems likely that the behavior reflects some  
514 other requirement of fly behavior, whose circuits are engaged by this stimulus. In this context,  
515 the anti-directional turning response represents a promising avenue to further constrain the  
516 underlying mechanisms of motion detection and integration. Indeed, just as illusory motion  
517 stimuli have placed key constraints on the circuits and algorithms for visual motion detection in  
518 flies and vertebrates (Agrochao et al., 2020; Clark *et al.*, 2011; Clark *et al.*, 2014; Eichner et al.,  
519 2011; Leonhardt *et al.*, 2016; Salazar-Gatzimas *et al.*, 2018; Salazar-Gatzimas *et al.*, 2016;  
520 Theobald et al., 2008; Tuthill et al., 2011) (Adelson and Bergen, 1985; Anstis and Rogers, 1975;  
521 Conway et al., 2005; Hassenstein and Reichardt, 1956; Hu and Victor, 2010; Livingstone et al.,  
522 2001; Livingstone and Conway, 2003; Mo and Koch, 2003; Orger et al., 2000), we believe that  
523 the anti-directional turning we describe here will provide additional insights.

524 In summary, we have presented evidence of a transition from syn-directional turning to no  
525 turning or to anti-directional turning when high contrast stimuli are presented to the fly. This  
526 persists across laboratory environments and across *Drosophila* species and shows plasticity with  
527 age. This behavior suggests that turning in response to rotational stimuli is not a simple reflex.  
528 Instead, the turning likely represents a superposition of behaviors driven by distinct circuits and  
529 elicited by different characteristics of the stimulus and different states of the fly. This complexity  
530 makes the optomotor response a model for studying the interactions of circuits as they control  
531 the low-dimensional behaviors that change an animal's orientation.

532

#### 533 **Contributions**

534 OM, MC, RT, MSC, NCBM, JS, and BAB collected data. OM, MC, TRC, and DAC wrote the  
535 paper.

536

537 **Acknowledgements**

538 This work was supported by NIH R01EY026555 (DAC), R01EY022638 (TRC), and by a Chan-  
539 Zuckerberg Investigator Award (TRC). MC was supported by an NDSEG Fellowship; RT was  
540 supported by the Takenaka Foundation; MSC was supported by an NSF GRFP; NCBM was  
541 supported by a CAPES fellowship; JS was supported by a Ford Foundation Fellowship.

542

543 **Methods**

544 **Fly strains**

545 Strains used in these experiments are listed in the tables below:

546 Table 1: Parental stock genotypes

Name	Genotype	Source	Stock #
Wildtype	+, +; + (IsoD1)	(Gohl et al., 2011)	N/A
T4T5-Gal4	+, +; R42F06-Gal4 (IsoD1 background)	BDSC	BDSC 41253
HS-Gal4	+, +; R27B03-Gal4 (IsoD1 bg)	(Seelig et al., 2010)	BDSC 49211
CH-Gal4	w; +; R35A10-Gal4 (Janelia bg)	BDSC	BDSC 49897
UAS-Shibire <sup>ts</sup>	+, +; UAS-Shibire <sup>ts</sup> (IsoD1 bg)	(Silies et al., 2013)	N/A
Empty Gal4	w; +; pBDPGAL4.1Uw (Janelia bg)	BDSC	BDSC 68384
GCaMP6f	w; UAS-GCaMP6f; +	BDSC	BDSC 42747
jGCaMP7b	w; +; UAS-jGCaMP7b	BDSC	BDSC 79029
mtdTomato	w; +; UAS-mtdTomato	BDSC	BDSC 30124

547

548 Table 2: Genotypes of flies used in behavior experiments

Experimental	Gal4 Control	UAS Control	Background Control
T4T5-Gal4 x UAS-Shibire <sup>ts</sup> ; +; +; R42F06-Gal4/UAS-Shibire <sup>ts</sup>	T4T5-Gal4 x IsoD1: +; +; R42F06-Gal4/+	IsoD1 x UAS-Shibire <sup>ts</sup> : +; +; +/UAS-Shibire <sup>ts</sup>	IsoD1: +; +; +
HS-Gal4 x UAS-Shibire <sup>ts</sup> ; +; +; R27B03-Gal4/UAS-Shibire <sup>ts</sup>	HS-Gal4 x IsoD1: +; +; R27B03-Gal4/+	IsoD1 x UAS-Shibire <sup>ts</sup> : +; +; +/UAS-Shibire <sup>ts</sup>	IsoD1: +; +; +
CH-Gal4 x UAS-Shibire <sup>ts</sup> ; w/+; +; R35A10-Gal4/UAS-Shibire <sup>ts</sup>	CH-Gal4 x IsoD1: w/+; +; R35A10-Gal4/+	Empty Gal4 x UAS-Shibire <sup>ts</sup> : +/w; +; pBDPGAL4.1Uw /UAS-Shibire <sup>ts</sup>	Empty Gal4 X IsoD1: +/w; +; +/- pBDPGAL4.1Uw

549

550 Genotypes of flies used in imaging experiments: +; +; HS-Gal4/UAS-jGCaMP7b, +; UAS-GC6f/+; T4T5-Gal4/UAS-mtdTomato, w/+; +; CH-Gal4/UAS-jGCaMP7b.

552 **Fly rearing (DAC lab)**

553 Unless otherwise noted, flies were reared at 20 degrees Celsius in Panasonic MIR-154-PA  
 554 incubators (Panasonic/PHC, Tokyo, Japan). The flies were circadian entrained on 12-hour light-  
 555 dark cycles. Flies were raised on Archon Scientific glucose food (recipe D20102, Archon  
 556 Scientific, Durham, NC). We used CO<sub>2</sub> to anesthetize flies more than 12 hours before the  
 557 behavioral experiments.

558 Flies were tested for behavior in rigs built in the labs of DAC and TRC. Behavior shown in **Figs.**  
 559 **1d, 1e, 6c, 6d, S1, and S4** was acquired in the lab of TRC, while the rest was obtained in the lab  
 560 of DAC.

561 **Fly rearing (TRC lab)**

562 Flies were reared at 25°C, on molasses-based food, and circadian entrained on 12-hour light-dark  
563 cycles. Flies were collected within three hours of eclosion using brief CO<sub>2</sub> anesthetization. *D.*  
564 *melanogaster* and *D. yakuba* were raised under identical conditions. Dark-reared flies were put  
565 in a dark chamber within 3 hours of eclosion. Flies tested at 0.5 days post eclosion were  
566 collected during the first two hours of the light cycle and were exposed to light until they were  
567 tested.

568

569 **Stimulus generation and behavioral turning assays (DAC lab)**

570 Stimuli were presented using DLP Lightcrafter (Texas Instruments, Dallas, TX) projectors  
571 (Creamer *et al.*, 2019). Mirrors were used to bounce the projected light onto three screens made  
572 of back-projection material, surrounding the fly. The screens covered the front 270 degrees  
573 around the fly, and ~45 degrees in elevation above and below the fly. The projectors were set to  
574 monochrome mode (green unless otherwise noted), updating at 180 Hz. Stimulus video was  
575 generated through a custom MATLAB (Mathworks, Natick, MA) application using  
576 PsychToolbox (Kleiner *et al.*, 2007). Stimuli were mapped onto a virtual cylinder around the fly  
577 and the MATLAB application generated a viewpoint-corrected video signal.

578 Behavioral experiments were performed 12-60 hours after staging. For behavioral experiments,  
579 we selected female flies, and co-housed them with males after staging. Flies were cold-  
580 anesthetized and fixed to needles using UV-cured epoxy (Norland optical adhesive #63, Norland  
581 Products, Cranbury, NJ). Flies were then placed above air-suspended polypropylene balls. These  
582 balls were 6 mm in diameter and weighed ~120 mg. The balls were painted with two layers of  
583 marker coatings- a base silver layer and a red top layer. The motion of balls was detected by  
584 either a Parallax mouse sensor board (Parallax, Rocklin, CA) with an MCS-12086 sensor (Unity  
585 Opto Technology, Taipei, Taiwan), or a custom board with an ADNS 2080 sensor (Avago  
586 Technologies / Broadcom Inc, San Jose, TX). The data from these sensors were transferred to a  
587 custom MATLAB application via an Arduino Uno board.

588 **Stimulus generation and behavioral turning assays (TRC lab)**

589 Stimuli were presented using a DLP Lightcrafter (Texas Instruments, Dallas, TX) projector.  
590 Three coherent optic fibers were used to direct the projected light onto three screens made of  
591 back-projection material, surrounding the fly (Clark *et al.*, 2011; Clark *et al.*, 2014). The screens  
592 covered the front 270 degrees around the fly, and ~45 degrees in elevation above and below the  
593 fly. The projectors were set to monochrome mode, updating at 120 Hz. Stimulus video was  
594 generated through Flystim (<https://github.com/ClandininLab/flystim>), a custom Python  
595 application developed in the Clandinin Lab (Turner *et al.*, 2022). Stimuli were mapped onto a  
596 virtual cylinder around the fly and Flystim generated a viewpoint-corrected video signal.

597 Behavioral experiments were performed 12-48 hours after eclosion, as described in the figures.  
598 Flies were cold-anesthetized and fixed to needles using UV-cured adhesive (Bondic, Niagara  
599 Falls, NY). Flies were then placed above air-suspended balls made with LAST-A-FOAM FR-  
600 4615 polyurethane foam (General Plastics, Tacoma, WA). These balls were 9 mm in diameter

601 and weighed ~91.7 mg. The motion of balls was detected by a Flea3 FL3-U3-13Y3M camera  
602 (Teledyne Flir, Wilsonville, OR) and Fictrac software (Moore et al., 2014).

### 603 **Imaging procedures**

604 Two photon imaging (**Fig. 5**) was performed as previously described (Tanaka and Clark, 2022).  
605 Briefly, two-photon images were acquired with a Scientifica microscope at between 6 and 13 Hz  
606 using a 930 nm femtosecond laser (SpectraPhysics, Santa Clara, USA) using ScanImage  
607 (Pologruto et al., 2003). Visual stimuli were presented on three screens occupying 270° of  
608 azimuthal angle about the fly using projectors (Creamer *et al.*, 2019). Optical filters on the  
609 projector and emission filters prevented the visual stimulus light from leaking into the two-  
610 photon images.

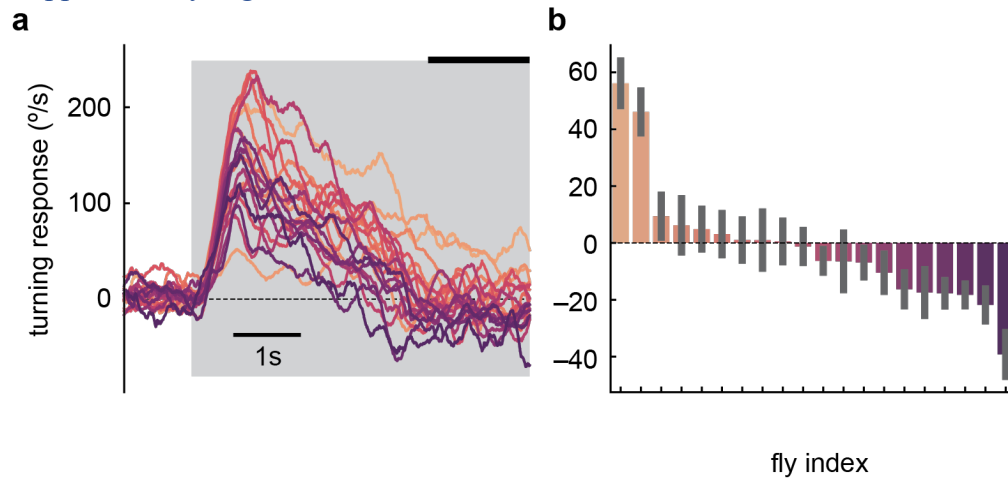
611 Regions of interest (ROIs) were extracted from image timeseries using a watershed algorithm.  
612 Responsive ROIs were included in the analyses. For T4 and T5 neurons, each ROI was identified  
613 as a T4-dominant or T5-dominant ROI by its response to light vs. dark edges, following prior  
614 procedures (Agrochao *et al.*, 2020). For all neuron types, responses were averaged over ROIs  
615 and over trials of each stimulus type to obtain a measurement for each fly; these fly  
616 measurements acted as the independent measurements to compute means and standard error bars  
617 for the figure.

### 618 **Statistical tests**

619 Throughout the paper, each fly was considered an independent sample for statistical purposes.  
620 Means and standard errors were computed over flies. For imaging experiments, regions of  
621 interest from a specific neuron type were first averaged within each fly, creating a value for each  
622 fly's response. These values were used to calculate means and standard errors over the tested  
623 flies. In the silencing experiments, a 2-sample Student t-test was used to test for significant  
624 differences between the experimental genotype and parental controls.

625

626 Supplementary Figures



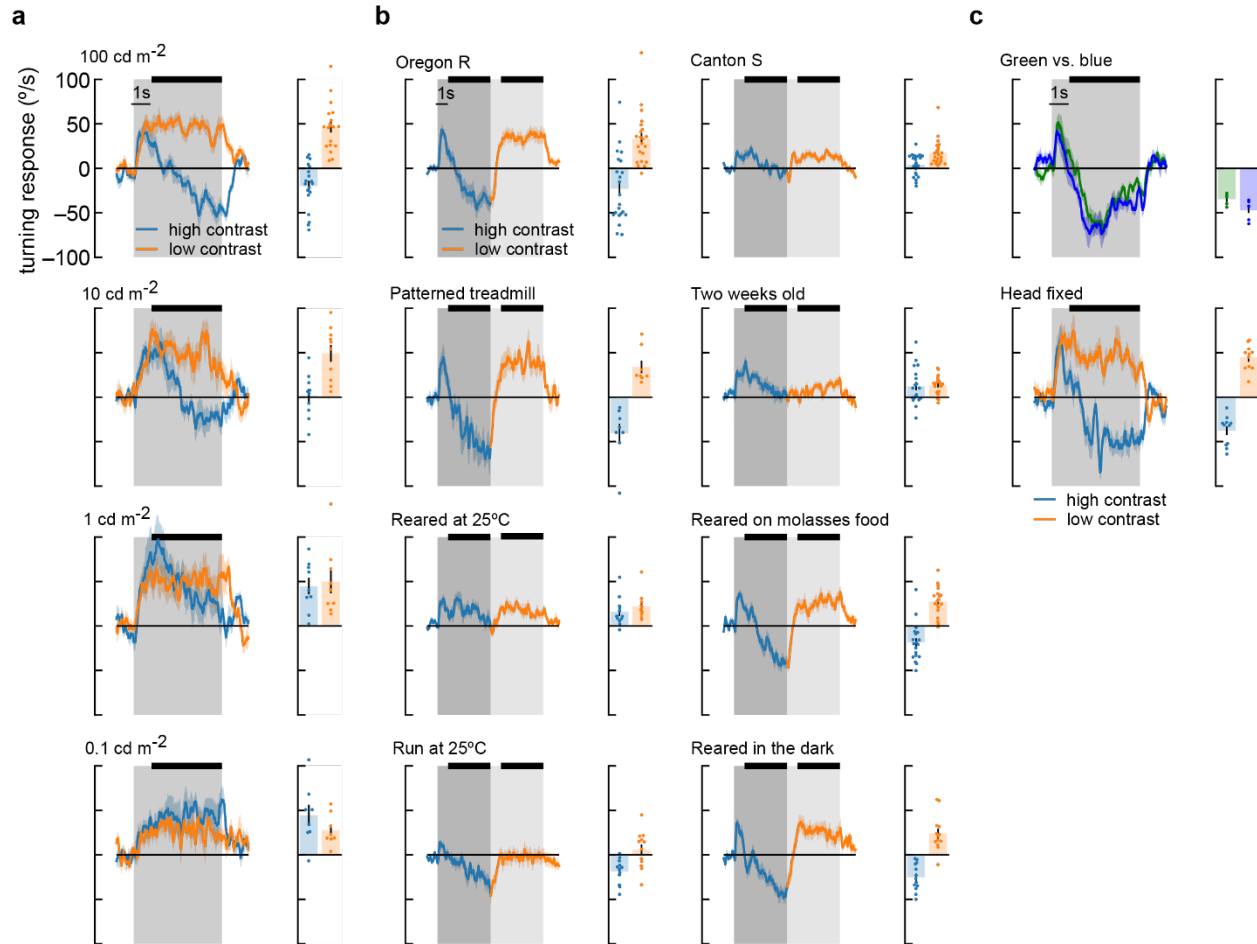
627

628 **Supplementary Figure S1. Individual *D. melanogaster* flies in TRC lab experiments show**  
629 **anti-directional turning.**

630 a) Mean time traces of individual fly responses to the high contrast stimulus, averaged over  
631 trials. The flies are those in **Fig. 1d**.

632 b) Long-timescale responses of individual flies, averaged over the last 1.5 s of the 5-second  
633 stimulus in panel (a) (indicated by thick black line). Mean and SEM shown are over the  
634 trials presented to that fly.

635



636

637 **Supplementary Figure S2. Flies perform anti-directional turning under a wide range of**  
 638 **stimulus and growing conditions.**

639 a) Fly turning behavior at different mean screen brightness. We swept brightness from 100  
 640 cd/m<sup>2</sup> to 0.1 cd/m<sup>2</sup> and measured turning responses to high and low contrast stimuli. Flies  
 641 performed the most anti-directional behavior in response to high brightness stimuli. At 1  
 642 cd/m<sup>2</sup>, flies never turned in the opposite direction of the stimulus, and at 0.1 cd/m<sup>2</sup>, flies  
 643 turned continuously in the same direction as the stimulus, even in high contrast  
 644 conditions. We also measured average turning during the last four seconds of stimulation  
 645 (black bar above time traces). Average fly behavior shown as bars on the right, with  
 646 individual fly behavior shown as dots. Shaded patches in the time trace plots represent ±1  
 647 SEM, as do vertical lines on bar plots. N = 19, 10, 9, 8 flies, top to bottom.

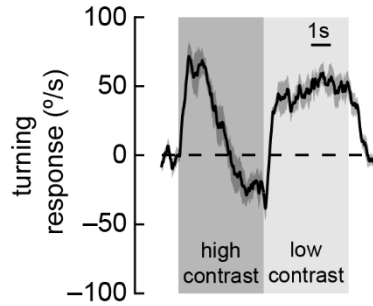
648 b) Our wildtype flies were Oregon-R strain (Gohl *et al.*, 2011) raised at 20 degrees. They  
 649 were grown on glucose-based food media with 12-hour light-dark cycles. Experiments  
 650 were run at high temperature, 12-60 hours after eclosion. We used uniform, red balls to  
 651 avoid visual feedback from walking. The response of these wildtype flies to a contrast-  
 652 switching stimulus (as in Fig. 2c) is shown in the upper left corner. We also tested  
 653 different variations of all these parameters. Canton-S flies turned less overall, and showed  
 654 less anti-directional turning, but still turned in the opposite direction after 5 seconds of



655 high contrast stimuli. We tested flies walking on highly-visible silver balls with black  
656 dots and saw behavior similar to wildtype. Two-week-old flies showed reduced turning  
657 and much reduced anti-directional behavior. Flies raised at 25 degrees Celsius had  
658 behavior similar to two-week-old flies. When we performed experiments at 25 degrees,  
659 we saw much less optomotor turning, but anti-directional turning persisted. Rearing on  
660 molasses-based media or in the dark did not have strong effects on behavior. N = 22, 8,  
661 12, 12, 24, 19, 19, 13 flies top to bottom, left to right.

662 **c)** Other changes to the experimental setup did not cause large differences in behavior. We  
663 compared responses to high contrast stimuli presented with green light (peak wavelength:  
664 525nm) and blue light (peak wavelength: 450), and did not see large differences in  
665 behavior. Head-fixed flies (middle) showed similar behavior to head-free flies (**a**, *top*). N  
666 = 5 and 11 flies, top to bottom.

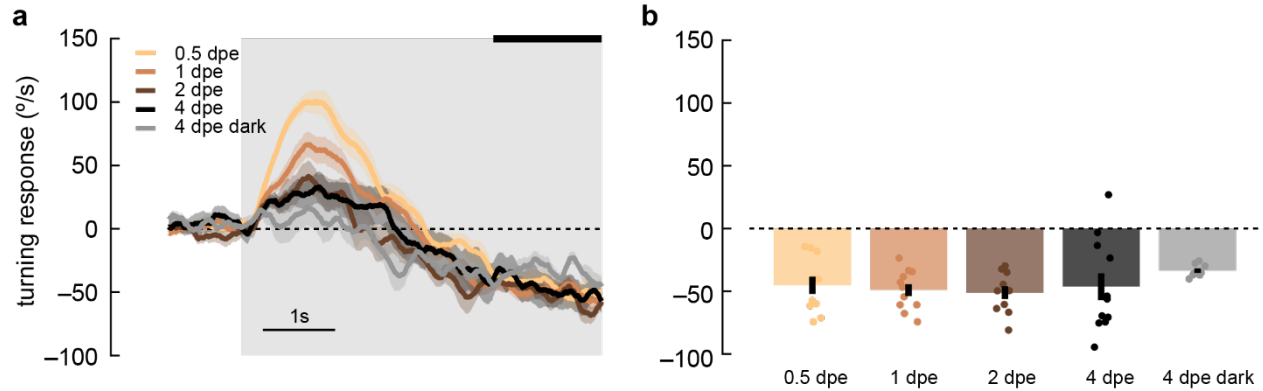
667



668

669 **Supplementary Figure S3. Anti-directional turning behavior occurs when using the optical**  
670 **filters also employed in the two-photon imaging experiments.** High and low contrast  
671 sinusoidal stimuli were presented as in Figure 2c, but using the bandpass filters also used in our  
672 two-photon microscope stimulus presentation. N = 30 flies.

673



674

675 **Supplementary Figure S4. *D. yakuba* lacks plasticity of anti-directional responses in**  
676 **adulthood that is observed *D. melanogaster*.**

- 677 a) Adult *yakuba* flies at various ages post eclosion were presented with 5-second, high-  
678 contrast, rotating sinusoidal gratings as in Fig. 6. Data was acquired in the TRC lab. Anti-  
679 directional responses stayed consistent from 0.5 days post eclosion (dpe) to 1, 2, and 4  
680 dpe, although the initial optomotor response became smaller as the flies aged. Shaded  
681 patches represent  $\pm 1$  SEM. N = 7-11 flies.
- 682 b) The last 1.5 seconds of the mean turning velocity of each fly was averaged, and the  
683 population response was plotted.

684

685 **Citations**

686

687 Adelson, E., and Bergen, J. (1985). Spatiotemporal energy models for the perception of motion.  
688 *JOSA A* 2, 284-299.

689 Agrochao, M., Tanaka, R., Salazar-Gatzimas, E., and Clark, D.A. (2020). Mechanism for  
690 analogous illusory motion perception in flies and humans. *Proc. Natl. Acad. Sci.* 117, 23044-  
691 23053.

692 Anstis, S.M., and Rogers, B.J. (1975). Illusory reversal of visual depth and movement during  
693 changes of contrast. *Vision Res.* 15, 957-966.

694 Arenz, A., Drews, M.S., Richter, F.G., Ammer, G., and Borst, A. (2017). The temporal tuning of  
695 the *Drosophila* motion detectors is determined by the dynamics of their input elements. *Curr.*  
696 *Biol.* 27, 929-944.

697 Bahl, A., Ammer, G., Schilling, T., and Borst, A. (2013). Object tracking in motion-blind flies.  
698 *Nat. Neurosci.* 16, 730-738.

699 Bahl, A., Serbe, E., Meier, M., Ammer, G., and Borst, A. (2015). Neural mechanisms for  
700 *Drosophila* contrast vision. *Neuron* 88, 1240-1252.

701 Barnhart, E.L., Wang, I.E., Wei, H., Desplan, C., and Clandinin, T.R. (2018). Sequential  
702 nonlinear filtering of local motion cues by global motion circuits. *Neuron* 100, 229-243. e223.

703 Bausenwein, B., Dittrich, A., and Fischbach, K.-F. (1992). The optic lobe of *Drosophila*  
704 *melanogaster*. *Cell Tissue Res.* 267, 17-28.

705 Behnia, R., Clark, D.A., Carter, A.G., Clandinin, T.R., and Desplan, C. (2014). Processing  
706 properties of ON and OFF pathways for *Drosophila* motion detection. *Nature* 512, 427-430.

707 Borst, A., and Weber, F. (2011). Neural Action Fields for Optic Flow Based Navigation: A  
708 Simulation Study of the Fly Lobula Plate Network. *PLOS ONE* 6, e16303.  
709 10.1371/journal.pone.0016303.

710 Bosch, D.S., van Swinderen, B., and Millard, S.S. (2015). *Dscam2* affects visual perception in  
711 *Drosophila melanogaster*. *Frontiers in behavioral neuroscience* 9, 149.

712 Buchner, E. (1976). Elementary movement detectors in an insect visual system. *Biol. Cybern.* 24,  
713 85-101.

714 Chiappe, M.E., Seelig, J.D., Reiser, M.B., and Jayaraman, V. (2010). Walking modulates speed  
715 sensitivity in *Drosophila* motion vision. *Curr. Biol.* 20, 1470-1475.

716 Clark, D. (1981). Visual responses in developing zebrafish. *Brachydanio rerio*.

717 Clark, D.A., Bursztyn, L., Horowitz, M.A., Schnitzer, M.J., and Clandinin, T.R. (2011). Defining  
718 the computational structure of the motion detector in *Drosophila*. *Neuron* 70, 1165-1177.

- 719 Clark, D.A., Fitzgerald, J.E., Ales, J.M., Gohl, D.M., Silies, M., Norcia, A.M., and Clandinin,  
720 T.R. (2014). Flies and humans share a motion estimation strategy that exploits natural scene  
721 statistics. *Nat. Neurosci.* *17*, 296-303.
- 722 Conway, B.R., Kitaoka, A., Yazdanbakhsh, A., Pack, C.C., and Livingstone, M.S. (2005). Neural  
723 basis for a powerful static motion illusion. *J. Neurosci.* *25*, 5651-5656.
- 724 Creamer, M.S., Mano, O., and Clark, D.A. (2018). Visual Control of Walking Speed in  
725 *Drosophila*. *Neuron* *100*, 1460-1473.
- 726 Creamer, M.S., Mano, O., Tanaka, R., and Clark, D.A. (2019). A flexible geometry for  
727 panoramic visual and optogenetic stimulation during behavior and physiology. *J. Neurosci.*  
728 *Methods* *323*, 48-55.
- 729 DeAngelis, B.D., Zavatone-Veth, J.A., and Clark, D.A. (2019). The manifold structure of limb  
730 coordination in walking *Drosophila*. *eLife* *8*, e46409.
- 731 Drews, M.S., Leonhardt, A., Pirogova, N., Richter, F.G., Schuetzenberger, A., Braun, L., Serbe,  
732 E., and Borst, A. (2020). Dynamic Signal Compression for Robust Motion Vision in Flies. *Curr.*  
733 *Biol.*
- 734 Duistermars, B., Chow, D., Condro, M., and Frye, M. (2007). The spatial, temporal and contrast  
735 properties of expansion and rotation flight optomotor responses in *Drosophila*. *J. Exp. Biol.* *210*,  
736 3218.
- 737 Eckert, H., and Dvorak, D.R. (1983). The centrifugal horizontal cells in the lobula plate of the  
738 blowfly, *Phaenicia sericata*. *J. Insect Physiol.* *29*, 547-560.
- 739 Eichner, H., Joesch, M., Schnell, B., Reiff, D.F., and Borst, A. (2011). Internal structure of the  
740 fly elementary motion detector. *Neuron* *70*, 1155-1164.
- 741 Frazor, R.A., and Geisler, W.S. (2006). Local luminance and contrast in natural images. *Vision*  
742 *Res.* *46*, 1585-1598.
- 743 Fujiwara, T., Brotas, M., and Chiappe, M.E. (2022). Walking strides direct rapid and flexible  
744 recruitment of visual circuits for course control in *Drosophila*. *Neuron*.
- 745 Goetz, K.G. (1968). Flight control in *Drosophila* by visual perception of motion. *Biol. Cybern.* *4*,  
746 199-208.
- 747 Gohl, D.M., Silies, M.A., Gao, X.J., Bhalerao, S., Luongo, F.J., Lin, C.C., Potter, C.J., and  
748 Clandinin, T.R. (2011). A versatile in vivo system for directed dissection of gene expression  
749 patterns. *Nat. Methods* *8*, 231-237.
- 750 Götz, K. (1964). Optomotorische untersuchung des visuellen systems einiger augenmutanten der  
751 fruchtfliege *Drosophila*. *Biol. Cybern.* *2*, 77-92.

- 752 Götz, K., and Wenking, H. (1973). Visual control of locomotion in the walking fruitfly  
753 *Drosophila*. *J. Comp. Physiol. A* *85*, 235-266.
- 754 Götz, K.G. (1970). Fractionation of *Drosophila* Populations According to Optomotor Traits.  
755 *Journal of Experimental Biology* *52*, 419-436.
- 756 Götz, K.G. (1975). The optomotor equilibrium of the *Drosophila* navigation system. *Journal of*  
757 *comparative physiology* *99*, 187-210. [10.1007/BF00613835](https://doi.org/10.1007/BF00613835).
- 758 Haikala, V., Joesch, M., Borst, A., and Mauss, A.S. (2013). Optogenetic control of fly optomotor  
759 responses. *J. Neurosci.* *33*, 13927-13934.
- 760 Hassenstein, B., and Reichardt, W. (1956). Systemtheoretische Analyse der Zeit-, Reihenfolgen-  
761 und Vorzeichenauswertung bei der Bewegungspertzeption des Rüsselkäfers *Chlorophanus*. *Zeits.*  
762 *Naturforsch.* *11*, 513–524.
- 763 Heisenberg, M., and Buchner, E. (1977). The role of retinula cell types in visual behavior  
764 of *Drosophila melanogaster*. *Journal of Comparative Physiology A: Neuroethology, Sensory,*  
765 *Neural, and Behavioral Physiology* *117*, 127-162.
- 766 Henning, M., Ramos-Traslosheros, G., Gür, B., and Silies, M. (2022). Populations of local  
767 direction-selective cells encode global motion patterns generated by self-motion. *Science*  
768 *advances* *8*, eabi7112.
- 769 Hu, Q., and Victor, J.D. (2010). A set of high-order spatiotemporal stimuli that elicit motion and  
770 reverse-phi percepts. *J. Vis.* *10*.
- 771 Joesch, M., Plett, J., Borst, A., and Reiff, D. (2008). Response properties of motion-sensitive  
772 visual interneurons in the lobula plate of *Drosophila melanogaster*. *Curr. Biol.* *18*, 368-374.
- 773 Joesch, M., Schnell, B., Raghu, S., Reiff, D., and Borst, A. (2010). ON and OFF pathways in  
774 *Drosophila* motion vision. *Nature* *468*, 300-304.
- 775 Juusola, M., Dau, A., Song, Z., Solanki, N., Rien, D., Jaciuch, D., Dongre, S.A., Blanchard, F.,  
776 de Polavieja, G.G., and Hardie, R.C. (2017). Microsaccadic sampling of moving image  
777 information provides *Drosophila* hyperacute vision. *Elife* *6*, e26117.
- 778 Katsov, A., and Clandinin, T. (2008). Motion processing streams in *Drosophila* are behaviorally  
779 specialized. *Neuron* *59*, 322-335.
- 780 Katsov, A.Y., Freifeld, L., Horowitz, M.A., Kuehn, S., and Clandinin, T.R. (2017). Dynamic  
781 structure of locomotor behavior in walking fruit flies. *eLife* *6*, e26410.
- 782 Ketkar, M.D., Sporar, K., Gür, B., Ramos-Traslosheros, G., Seifert, M., and Silies, M. (2020).  
783 Luminance information is required for the accurate estimation of contrast in rapidly changing  
784 visual contexts. *Curr. Biol.* *30*, 657-669. e654.

- 785 Kim, A.J., Fenk, L.M., Lyu, C., and Maimon, G. (2017). Quantitative predictions orchestrate  
786 visual signaling in *Drosophila*. *Cell* *168*, 280-294. e212.
- 787 Kiral, F.R., Dutta, S.B., Linneweber, G.A., Hilgert, S., Poppa, C., Duch, C., von Kleist, M.,  
788 Hassan, B.A., and Hiesinger, P.R. (2021). Brain connectivity inversely scales with  
789 developmental temperature in *Drosophila*. *Cell Rep.* *37*, 110145.
- 790 Kitamoto, T. (2001). Conditional modification of behavior in *Drosophila* by targeted expression  
791 of a temperature-sensitive shibire allele in defined neurons. *J. Neurobiol.* *47*, 81-92.
- 792 Kleiner, M., Brainard, D., Pelli, D., Ingling, A., Murray, R., and Broussard, C. (2007). What's  
793 new in Psychtoolbox-3. *Perception* *36*, 1.
- 794 Koerner, F., and Schiller, P.H. (1972). The optokinetic response under open and closed loop  
795 conditions in the monkey. *Exp. Brain Res.* *14*, 318-330.
- 796 Krapp, H.G., and Hengstenberg, R. (1996). Estimation of self-motion by optic flow processing in  
797 single visual interneurons. *Nature* *384*, 463-466.
- 798 Leong, J.C.S., Esch, J.J., Poole, B., Ganguli, S., and Clandinin, T.R. (2016). Direction selectivity  
799 in *Drosophila* emerges from preferred-direction enhancement and null-direction suppression. *J.*  
800 *Neurosci.* *36*, 8078-8092.
- 801 Leonhardt, A., Ammer, G., Meier, M., Serbe, E., Bahl, A., and Borst, A. (2016). Asymmetry of  
802 *Drosophila* ON and OFF motion detectors enhances real-world velocity estimation. *Nat.*  
803 *Neurosci.* *19*, 706–715.
- 804 Livingstone, M., Pack, C., and Born, R. (2001). Two-dimensional substructure of MT receptive  
805 fields. *Neuron* *30*, 781-793.
- 806 Livingstone, M.S., and Conway, B.R. (2003). Substructure of direction-selective receptive fields  
807 in macaque V1. *J. Neurophysiol.* *89*, 2743-2759.
- 808 Maisak, M.S., Haag, J., Ammer, G., Serbe, E., Meier, M., Leonhardt, A., Schilling, T., Bahl, A.,  
809 Rubin, G.M., Nern, A., et al. (2013). A directional tuning map of *Drosophila* elementary motion  
810 detectors. *Nature* *500*, 212-216.
- 811 Matulis, C.A., Chen, J., Gonzalez-Suarez, A., Behnia, R., and Clark, D.A. (2020).  
812 Heterogeneous temporal contrast adaptation in *Drosophila* direction-selective circuits. *Curr. Biol.*
- 813 Mauss, A.S., Pankova, K., Arenz, A., Nern, A., Rubin, G.M., and Borst, A. (2015). Neural  
814 circuit to integrate opposing motions in the visual field. *Cell* *162*, 351-362.
- 815 McCann, G.D., and MacGinitie, G. (1965). Optomotor response studies of insect vision.  
816 *Proceedings of the Royal Society of London. Series B. Biological Sciences* *163*, 369-401.
- 817 Mo, C.-H., and Koch, C. (2003). Modeling reverse-phi motion-selective neurons in cortex:  
818 double synaptic-veto mechanism. *Neural Comput.* *15*, 735-759.

- 819 Mongeau, J.-M., and Frye, M.A. (2017). *Drosophila* spatiotemporally integrates visual signals to  
820 control saccades. *Curr. Biol.* 27, 2901-2914. e2902.
- 821 Moore, R.J., Taylor, G.J., Paulk, A.C., Pearson, T., van Swinderen, B., and Srinivasan, M.V.  
822 (2014). FicTrac: a visual method for tracking spherical motion and generating fictive animal  
823 paths. *J. Neurosci. Methods* 225, 106-119.
- 824 Orger, M.B., Smear, M.C., Anstis, S.M., and Baier, H. (2000). Perception of Fourier and non-  
825 Fourier motion by larval zebrafish. *Nat. Neurosci.* 3, 1128-1133.
- 826 Pologruto, T.A., Sabatini, B.L., and Svoboda, K. (2003). ScanImage: flexible software for  
827 operating laser scanning microscopes. *Biomed. Eng. Online* 2, 13.
- 828 Rister, J., Pauls, D., Schnell, B., Ting, C., Lee, C., Sinakevitch, I., Morante, J., Strausfeld, N.,  
829 Ito, K., and Heisenberg, M. (2007). Dissection of the peripheral motion channel in the visual  
830 system of *Drosophila melanogaster*. *Neuron* 56, 155-170.
- 831 Rivlin-Etzion, M., Wei, W., and Feller, M.B. (2012). Visual stimulation reverses the directional  
832 preference of direction-selective retinal ganglion cells. *Neuron* 76, 518-525.
- 833 Salazar-Gatzimas, E., Agrochao, M., Fitzgerald, J.E., and Clark, D.A. (2018). The Neuronal  
834 Basis of an Illusory Motion Percept Is Explained by Decorrelation of Parallel Motion Pathways.  
835 *Curr. Biol.* 28, 3748-3762. e3748.
- 836 Salazar-Gatzimas, E., Chen, J., Creamer, M.S., Mano, O., Mandel, H.B., Matulis, C.A.,  
837 Pottackal, J., and Clark, D.A. (2016). Direct measurement of correlation responses in *Drosophila*  
838 elementary motion detectors reveals fast timescale tuning. *Neuron* 92, 227-239.
- 839 Schilling, T., and Borst, A. (2015). Local motion detectors are required for the computation of  
840 expansion flow-fields. *Biology open*, bio. 012690.
- 841 Schnell, B., Raghu, S.V., Nern, A., and Borst, A. (2012). Columnar cells necessary for motion  
842 responses of wide-field visual interneurons in *Drosophila*. *J. Comp. Physiol. A* 198, 389-395.
- 843 Schweigart, G., Mergner, T., Evdokimidis, I., Morand, S., and Becker, W. (1997). Gaze  
844 stabilization by optokinetic reflex (OKR) and vestibulo-ocular reflex (VOR) during active head  
845 rotation in man. *Vision Res.* 37, 1643-1652.
- 846 Seelig, J., Chiappe, M., Lott, G., Dutta, A., Osborne, J., Reiser, M., and Jayaraman, V. (2010).  
847 Two-photon calcium imaging from head-fixed *Drosophila* during optomotor walking behavior.  
848 *Nat. Methods*.
- 849 Shinomiya, K., Huang, G., Lu, Z., Parag, T., Xu, C.S., Aniceto, R., Ansari, N., Cheatham, N.,  
850 Lauchie, S., Neace, E., et al. (2019). Comparisons between the ON-and OFF-edge motion  
851 pathways in the *Drosophila* brain. *eLife* 8, e40025.
- 852 Silies, M., Gohl, D.M., Fisher, Y.E., Freifeld, L., Clark, D.A., and Clandinin, T.R. (2013).  
853 Modular use of peripheral input channels tunes motion-detecting circuitry. *Neuron* 79, 111-127.



- 854 Strother, J.A., Nern, A., and Reiser, M.B. (2014). Direct observation of ON and OFF pathways  
855 in the *Drosophila* visual system. *Curr. Biol.* *24*, 976-983.
- 856 Strother, J.A., Wu, S.-T., Rogers, E.M., Eliason, J.L., Wong, A.M., Nern, A., and Reiser, M.B.  
857 (2018). Behavioral state modulates the ON visual motion pathway of *Drosophila*. *Proc. Natl.*  
858 *Acad. Sci. USA* *115*, E102-E111.
- 859 Strother, J.A., Wu, S.-T., Wong, A.M., Nern, A., Rogers, E.M., Le, J.Q., Rubin, G.M., and  
860 Reiser, M.B. (2017). The emergence of directional selectivity in the visual motion pathway of  
861 *Drosophila*. *Neuron* *94*, 168-182. e110.
- 862 Takemura, S.-y., Bharioke, A., Lu, Z., Nern, A., Vitaladevuni, S., Rivlin, P.K., Katz, W.T.,  
863 Olbris, D.J., Plaza, S.M., Winston, P., et al. (2013). A visual motion detection circuit suggested  
864 by *Drosophila* connectomics. *Nature* *500*, 175-181.
- 865 Tammero, L., Frye, M., and Dickinson, M. (2004). Spatial organization of visuomotor reflexes in  
866 *Drosophila*. *J. Exp. Biol.* *207*, 113-122.
- 867 Tanaka, R., and Clark, D.A. (2022). Neural mechanisms to exploit positional geometry for  
868 collision avoidance. *Curr. Biol.* *32*, 2357-2374.e2356.
- 869 Theobald, J.C., Duistermars, B.J., Ringach, D.L., and Frye, M.A. (2008). Flies see second-order  
870 motion. *Curr. Biol.* *18*, R464-R465.
- 871 Turner, M.H., Krieger, A., Pang, M.M., and Clandinin, T.R. (2022). Visual and motor signatures  
872 of locomotion dynamically shape a population code for visual features in *Drosophila*. bioRxiv.
- 873 Tuthill, J.C., Chiappe, M.E., and Reiser, M.B. (2011). Neural correlates of illusory motion  
874 perception in *Drosophila*. *Proc. Natl. Acad. Sci. USA* *108*, 9685-9690.
- 875 Tuthill, J.C., Nern, A., Holtz, S.L., Rubin, G.M., and Reiser, M.B. (2013). Contributions of the  
876 12 neuron classes in the fly lamina to motion vision. *Neuron* *79*, 128-140.
- 877 Vlasits, A.L., Bos, R., Morrie, R.D., Fortuny, C., Flannery, J.G., Feller, M.B., and Rivlin-Etzion,  
878 M. (2014). Visual stimulation switches the polarity of excitatory input to starburst amacrine  
879 cells. *Neuron* *83*, 1172-1184.
- 880 Wei, H., Kyung, H.Y., Kim, P.J., and Desplan, C. (2020). The diversity of lobula plate tangential  
881 cells (LPTCs) in the *Drosophila* motion vision system. *J. Comp. Physiol. A* *206*, 139-148.
- 882 Wienecke, C.F., Leong, J.C., and Clandinin, T.R. (2018). Linear Summation Underlies Direction  
883 Selectivity in *Drosophila*. *Neuron*.
- 884 Williamson, W.R., Peek, M.Y., Breads, P., Coop, B., and Card, G.M. (2018). Tools for Rapid  
885 High-Resolution Behavioral Phenotyping of Automatically Isolated *Drosophila*. *Cell Rep.* *25*,  
886 1636-1649. e1635.

- 887 Wolf, R., and Heisenberg, M. (1990). Visual control of straight flight in *Drosophila*  
888 *melanogaster*. *Journal of Comparative Physiology A: Neuroethology, Sensory, Neural, and*  
889 *Behavioral Physiology* *167*, 269-283.
- 890 Yang, H.H., and Clandinin, T.R. (2018). Elementary motion detection in *Drosophila*: algorithms  
891 and mechanisms. *Ann. Rev. Vis. Sci.* *4*, 143-163.
- 892 York, R.A., Brezovec, L.E., Coughlan, J., Herbst, S., Krieger, A., Lee, S.-Y., Pratt, B., Smart,  
893 A.D., Song, E., and Suvorov, A. (2022). The evolutionary trajectory of drosophilid walking.  
894 *Curr. Biol.*
- 895